Carbohydrate-like composition of submicron atmospheric particles and their production from ocean bubble bursting

Lynn M. Russell[a,1], Lelia N. Hawkins[a], Amanda A. Frossard[a], Patricia K. Quinn[b], and Tim S. Bates[b]

[a]Scripps Institution of Oceanography, University of California San Diego, La Jolla, California 92093 [b]Pacific Marine Environmental Laboratory, National Oceanic and Atmospheric Administration, Seattle, Washington 98115

Edited by Barbara J. Finlayson-Pitts, University of California, Irvine, CA, and approved November 6, 2009 (received for review August 6, 2009)

Oceans cover over two-thirds of the Earth's surface, and the particles emitted to the atmosphere by waves breaking on sea surfaces provide an important contribution to the planetary albedo. During the International Chemistry Experiment in the Arctic LOwer Troposphere (ICEALOT) cruise on the R/V *Knorr* in March and April of 2008, organic mass accounted for 15–47% of the submicron particle mass in the air masses sampled over the North Atlantic and Arctic Oceans. A majority of this organic component ($0.1 - 0.4\ \mu m^{-3}$) consisted of organic hydroxyl (including polyol and other alcohol) groups characteristic of saccharides, similar to biogenic carbohydrates found in seawater. The large fraction of organic hydroxyl groups measured during ICEALOT in submicron atmospheric aerosol exceeded those measured in most previous campaigns but were similar to particles in marine air masses in the open ocean (Southeast Pacific Ocean) and coastal sites at northern Alaska (Barrow) and northeastern North America (Appledore Island and Chebogue Point). The ocean-derived organic hydroxyl mass concentration during ICEALOT correlated strongly to submicron Na concentration and wind speed. The observed submicron particle ratios of marine organic mass to Na were enriched by factors of $\sim 10^2$–$\sim 10^3$ over reported sea surface organic to Na ratios, suggesting that the surface-controlled process of film bursting is influenced by the dissolved organic components present in the sea surface microlayer. Both marine organic components and Na increased with increasing number mean diameter of the accumulation mode, suggesting a possible link between organic components in the ocean surface and aerosol–cloud interactions.

atmospheric aerosol | marine carbohydrates | organic aerosols | sea salt particles

The scattering of light by salt aerosol particles over the ocean remains an important and uncertain part of climate models (1). Recent observations quantifying the submicron salt particle flux suggest that submicron sea salt particles could account for as much as 90% of cloud condensation nuclei (CCN) in marine regions with little continental influence (2). Discrepancies between observed and modeled organic carbon in aerosol particles at marine sites have resulted in the attribution of $0.1 - 0.5\ \mu g\ C\ m^{-3}$ to primary (directly emitted) or secondary (atmospherically processed) oceanic sources for three coastal sites in the North Atlantic in the months of March and April (3). The chemical composition of particles from such marine organic compounds may influence cooling or warming at the top of the atmosphere, depending on the optical characteristics of these compounds, which remain uncertain (4). Some of this uncertainty results from the poor chemical characterization of the organic compounds emitted with salt as a result of wave-breaking processes, precluding incorporation of particle hygroscopic and surface tension properties in models of their effects on clouds and radiative transfer (5, 6).

Gagosian et al. (7) showed the presence of alcohols, fatty acid salts, and esters as specific tracers of ocean-derived organic compounds in atmospheric aerosol particles collected in a pristine region of the Pacific Ocean. These compounds included saccharides, fatty acids, and a few other organic classes. Recent improvements in analytical techniques have extended the range of individual compounds identified in ocean-derived aerosol particles to include high molecular weight, partially oxidized biological compounds like monosaccharides and polysaccharides, fatty acids and alcohols, amines, and amino acids (8–17). The biological source of some of these compounds has been supported by correspondence to satellite metrics of high chlorophyll regions (15, 16, 18), and some of these compounds may originate from components of biological organisms or particulate organic carbon (POC) (14, 19).

Mochida et al. (15) note that the low molecular weight saturated fatty acids that they analyzed account for at most 4% of the organic compounds in marine films. Aluwihare et al. (20) have provided some information on what the remaining marine organic components might be by showing that carbohydrates constitute 80% of seawater dissolved organic carbon (DOC). Their work has shown that some of these carbohydrates may be part of microorganisms, but that a majority of the components are their metabolites or by-products (21). Because these components constitute a large fraction of seawater organic carbon, we expect that they also constitute a large fraction of submicron atmospheric particles derived from ocean sources. Crahan et al. (10) have provided evidence for significant concentrations of glucose and other carbohydrates in ocean-derived atmospheric particles, identifying 7–20% of organic mass (OM) as marine carbohydrates in aerosol particles. If seawater DOC is the source of organic components in marine particles, then we expect that their composition would be similar to 80% carbohydrates, but the remaining carbohydrate compounds have not been identified.

In this work, we identify a consistent, carbohydrate-like, ocean-derived organic signature by Fourier Transform Infrared (FTIR) spectroscopy that accounts for 68% and 37%, respectively, of the organic mass of submicron aerosol particles collected on the R/V *Knorr* in the North Atlantic and Arctic Ocean regions. This fraction of OM is significant because in these clean, marine regions, it accounts for 7–37% of submicron particle mass. This marine particle signature is also evident in measurements from a clean region of the Southeast Pacific [during the VAMOS Ocean-Cloud-Atmosphere-Land Study Regional Experiment (VOCALS-REx), in 2008] and at Barrow (on the northern coast of Alaska). Single particle measurements show organic groups on crystallized salts, providing evidence that soluble organic components are

Author contributions: L.M.R., P.K.Q., and T.S.B. designed research; L.M.R., P.K.Q., and T.S.B. performed research; L.M.R. and A.A.F. contributed new reagents/analytic tools; L.M.R., L.N.H., and A.A.F. analyzed data; L.M.R. wrote the paper; and P.K.Q. and T.S.B. provided revisions to the paper.

The authors declare no conflict of interest.

This article is a PNAS Direct Submission.

[1]To whom correspondence should be addressed. E-mail: lmrussell@ucsd.edu.

This article contains supporting information online at www.pnas.org/cgi/content/full/0908905107/DCSupplemental.

internally mixed with sea salts. Using quantitative correlations of the measured marine particles, we discuss the correlation of the submicron marine organic particle mass concentration with wind speed and the relationships of submicron marine particle OM, Na, and particle diameter in order to assess the characteristics and production of submicron ocean-derived atmospheric particles. We show that the enrichment of the marine fraction of organic mass with respect to sea salt is regionally variable but consistent with surface-active compounds influencing the film-breaking processes that form submicron marine particles.

Results

The measured submicron OM (OM1) concentration was <0.5 μg m^{-3} for much of the International Chemistry Experiment in the Arctic LOwer Troposphere (ICEALOT) cruise over the more remote open ocean regions in the North Atlantic and Arctic, indicating little influence of continental emissions. This OM1 constituted up to $1/3$ of the submicron particle mass (PM1). In coastal and other continentally influenced areas, OM1 concentration reached between 1 and 2 μg m^{-3}. This analysis focuses on the regions of the cruise with minimal influence of continental emissions, as determined by back trajectories and radon concentrations (see Fig. S1 and Table S1). In this section, we discuss six independent pieces of observational evidence that identify 30–50% of OM1 in these sectors (in the North Atlantic and Arctic regions) as marine in origin. Because submicron particles are produced by bursting of the bubble films formed by wave-breaking, the organic hydroxyl groups from carbohydrates that constitute almost 90% of the organic mass of the ocean-derived atmospheric particles are likely emitted by the same bubble-bursting process.

Observed Organic Hydroxyl Groups, NaCl, and Wind Speed. The most striking feature of the ICEALOT organic functional group composition with respect to measurements in other regions (22–24) is the abundance of organic hydroxyl functional group mass during the ICEALOT campaign, accounting for 47% of OM1 on average (see Table S1). This feature is more pronounced in the North Atlantic and Arctic air masses that had some of the lowest OM1 and PM1 concentrations but the highest fractions of organic hydroxyl groups compared to other coastal or open ocean campaigns, as shown in the pie charts in Fig. 1. In these air masses, the average organic hydroxyl group mass contributions were 61% and 47% of the OM1 for the North Atlantic and Arctic, respectively (as summarized in Table S1). The organic hydroxyl concentration in the clean sectors was correlated to the submicron Na (Na1) concentration with r = 0.74 in the North Atlantic and r = 0.89 in the Arctic, as shown in Fig. 2*A*. (Na1 matches Cl1 on a molar basis for the duration of the North Atlantic and Arctic sampling and is used here as a convenient proxy for submicron NaCl and subsequently sea salt.) Because Na1 is known to form primary particles from evaporating seawater droplets, the close correlation of organic components with Na1 suggests their direct association and probable primary formation. Positive correlations of Na with fatty acids within aerosol particles were found by Pelzer et al. (24) and Mochida et al. (15) for pristine regions. In addition, Crahan et al. (10) found a correlation between carbohydrates and Na concentration for particles of marine origin in the Northeastern Pacific. However, this paper presents the identification of significant organic mass concentrations (exceeding 0.2 μg m^{-3} and >50% of OM1) correlated to Na1, owing to both the windy, pristine marine conditions reducing other organic components and the ability of FTIR to identify a large fraction of the particle organic mass without separation or contamination by extraction.

Because salt spray particles are produced by the mechanical action of breaking waves and consequent bubble bursting, correlations of submicron and supermicron particle number, mass, and NaCl to locally observed simultaneous wind speeds have been used to attribute their origin to marine sources (25). However, because wind speed controls the local flux rather than local concentration of marine particles (26), a strong relationship to wind

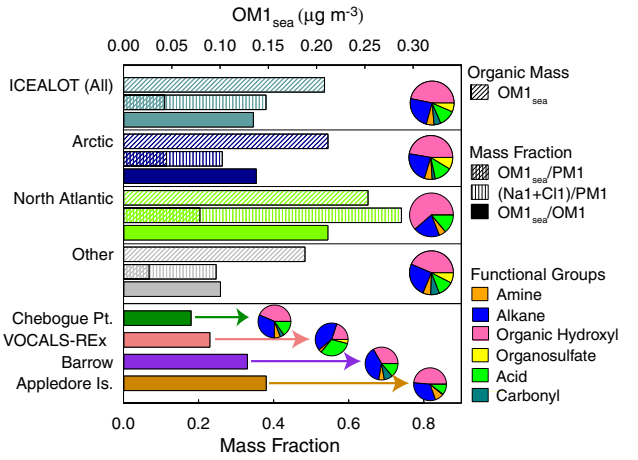

Fig. 1. Contribution of $OM1_{sea}$ to OM1 (solid bars, bottom axis) for the Arctic, North Atlantic, and Other samples as well as the entire ICEALOT campaign, with project averages for Chebogue Point (ICARTT), VOCALS-REx, Barrow (2008), and Appledore Island (ICARTT) shown below. For the ICEALOT sectors of Arctic (*dark blue*), North Atlantic (*chartreuse*), and Other (*gray*), the middle bar shows the contribution of $OM1_{sea}$ (at left, cross-hatched) and submicron NaCl (at right, vertical lines) as mass fractions of PM1 (bottom axis) and the top bar (with diagonal lines) shows $OM1_{sea}$ concentration (top axis). Pie charts at right show the average FTIR functional group composition for each project and sector, where colors indicate organic hydroxyl (*hot pink*), alkane (*blue*), carboxylic acid (*green*), amine (*orange*), nonacidic carbonyl (*teal*), and organosulfate (*yellow*) groups as fractions of OM1, as shown in the legend.

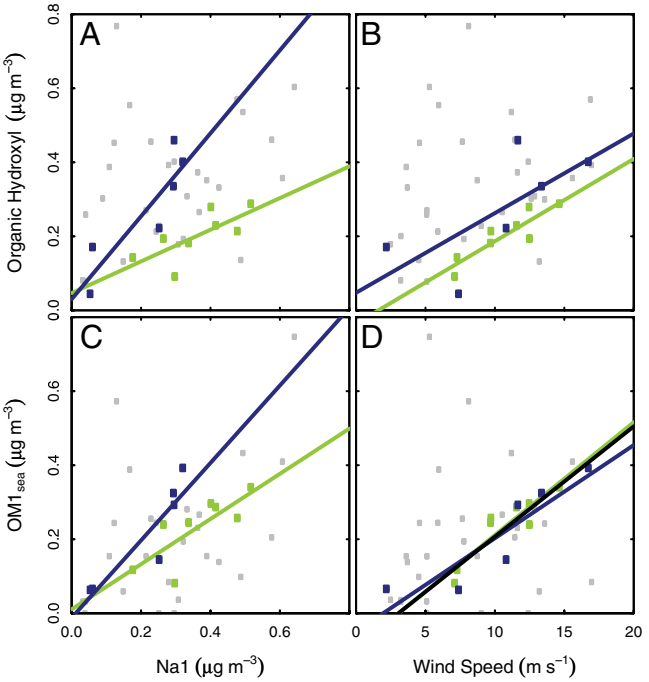

Fig. 2. Dependence of concentration of FTIR organic hydroxyl group concentration on (*A*) Na1 concentration (r = 0.74 for North Atlantic; r = 0.89 for Arctic; r = 0.30 for all), (*B*) wind speed (r = 0.89 for North Atlantic; r = 0.70 for Arctic; r = 0.26 for all), and dependence of concentration of PMF marine factor $OM1_{sea}$ on (*C*) Na1 concentration (r = 0.78 for North Atlantic; r = 0.91 for Arctic; r = 0.51 for all), (*D*) wind speed (r = 0.91 for North Atlantic; r = 0.90 for Arctic; r = 0.30 for all). Symbols and fit lines (with coefficients given in Table S3) are colored by sector as in Fig. 1; black line in (*D*) is the fit for both North Atlantic and Arctic sectors together, as given in Eq. [**1**].

speed would require regional homogeneity of wind speed or dominance of the concentration by recent emissions (which is typically a more reasonable assumption for shorter-lived, larger particles). During ICEALOT in the North Atlantic, submicron and supermicron Na concentrations are only mildly correlated to wind speed ($r = 0.63$ and $r = 0.75$, respectively), where the lower correlation in the supermicron particles may result from the greater variability in sampling conditions during the stormy North Atlantic crossing. However, in the Arctic regions there were strong correlations of submicron and supermicron Na with wind speed ($r = 0.90$ and $r = 0.87$, respectively). As shown in Fig. 2*B*, correlations of organic hydroxyl group concentrations to wind speed were mild in the Arctic ($r = 0.70$) and strong for the North Atlantic ($r = 0.89$). The correlations of organic hydroxyl concentrations with wind speed are surprisingly strong, given that nonlocal particle fluxes (emitted in regions with different wind speeds) and nonmarine organic hydroxyl sources may contribute to the variability and reduce the strength of the correlation. The regional differences in both correlations and slopes could result from differences in local wind speeds, the DOC and POC composition of the surface seawater, and the potential contribution of particles released from frost flowers on sea ice-covered regions of the Arctic. Ratios of organic hydroxyl concentrations to Na are higher in the Arctic than the North Atlantic by a factor of 2, although the slopes of organic hydroxyl concentration with wind speed are very similar.

Carbohydrate-Like Composition of Marine Organic Hydroxyl Factor. Positive matrix factorization (PMF) was used to extract the source-specific components of the FTIR spectra from 1,500 to 4,000 cm^{-1}wavenumbers, using the procedure of Russell et al. (27). PMF results for 2–6 factors were analyzed, and the 4-factor solution was chosen because it represented the variability of the measurements well ($r = 0.93$), and the residuals were $<1/2$ of the intrinsic uncertainty of the measurements. One feature was robust among the results for 2, 3, 4, 5, and 6 factors: the identification of a factor with 70–90% organic hydroxyl groups and with weak ($0.25 < r < 0.50$) or mild ($0.50 < r < 0.75$) correlations with submicron Na concentration. The marine factor in the 4-factor PMF results has 88% organic hydroxyl group mass fraction (shown in Fig. 3) and was correlated mildly to submicron Na (Na1, $r = 0.51$) and Cl (Cl1, $r = 0.56$) concentration and weakly to submicron K ($r = 0.44$) and supermicron Na ($r = 0.41$) for all samples in the ICEALOT project. The calculated FTIR spectrum for this factor is similar to both reference saccharides and marine factors identified in other campaigns, as shown in Fig. 3 (see *SI Text*, specifically Table S2). In the North Atlantic and Arctic air masses, this marine factor OM1 ($OM1_{sea}$) concentration accounts for up to 0.4 $\mu g\, m^{-3}$ and correlates to Na1 concentration as illustrated in Fig. 2*C*, and its correlation with wind speed is shown in Fig. 2*D*. The results show stronger correlations of the marine factor $OM1_{sea}$ than with organic hydroxyl concentration for wind speed in both regions, with $r = 0.91$ for North Atlantic and $r = 0.90$ for Arctic. The correlations of $OM1_{sea}$ with Na1 are nominally increased for the Arctic (from $r = 0.89$ to $r = 0.91$) and in the North Atlantic (from $r = 0.74$ to $r = 0.78$). The improvements show that the Na-correlated marine factor is a better proxy for quantifying the marine-origin OM than the entirety of the organic hydroxyl groups, even though the latter constitutes 88% of the PMF-based $OM1_{sea}$.

To identify the potential source regions of the high organic hydroxyl mass fraction and the $OM1_{sea}$/OM1, we have used hybrid single particle langrangian integrated trajectory (HYSPLIT) back trajectories with gridded frequencies of co-occurrence with high concentration measurements (> the 75th percentile value for the project), using an algorithm known as Potential Source Contribution Function (PSCF), shown in Fig. 4*A* and *B* (*SI Text*). Three source regions identified both for the high organic

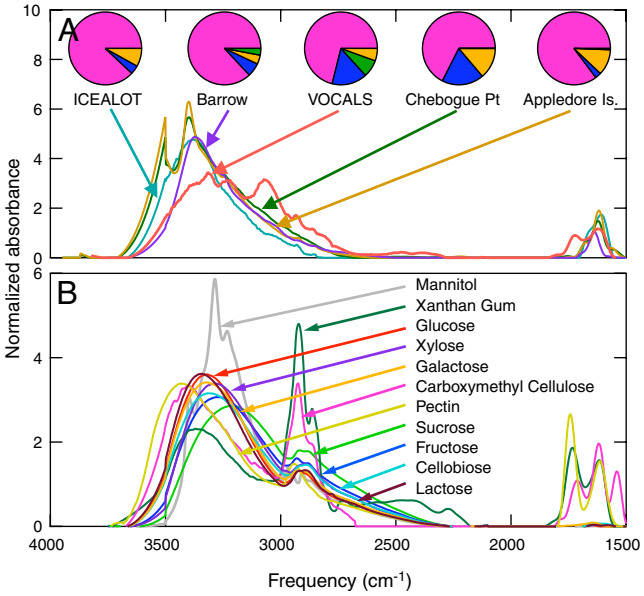

Fig. 3. FTIR spectra of (*A*) PMF-based marine factors for ICEALOT, VOCALS-REx, Barrow (winter), Chebogue Point (ICARTT), and Appledore Island (ICARTT) and (*B*) selected reference standards for saccharides as listed. The pie charts in (*A*) show the average composition of each of the marine factor FTIR spectra shown.

hydroxyl fractions and the high $OM1_{sea}$ concentrations are collocated, with a strong and dispersed signature in the northwestern Atlantic, a more condensed region of the northeastern Atlantic, and a third weaker signature associated with the lower concentrations measured in the Arctic Ocean northeast of Iceland. The PSCF confirms that the likely sources of much of the organic hydroxyl are in the ocean rather than from long-range transport of biomass burning or other continental particle emissions, both of which are unlikely due to the lack of tracers for either combustion or biogenic processes.

Organic Components on NaCl Particles. To further test the hypothesis that the marine factor organic components are emitted as primary particles from organic-containing seawater, we looked for evidence of individual particles containing mixtures of organic hydroxyl groups and NaCl. Of the 43 carbon-containing particles analyzed by scanning transmission x-ray microscopy near edge x-ray absorption fine structure (STXM-NEXAFS) from in or near the Arctic air masses of ICEALOT, 26 particles had cuboidal

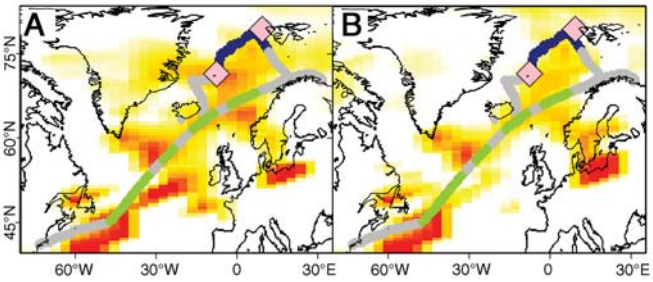

Fig. 4. ICEALOT regional maps of potential source contribution functions for (*A*) organic hydroxyl group mass fractions of OM1 and (*B*) $OM1_{sea}$/OM1. The colored lines show the cruise track, with colors indicating air mass sectors as in Fig. 1. The high probability potential source regions are colored dark red with lower probabilities in yellow. The pink diamond markers represent the locations of particles sampled for STXM-NEXAFS and EDX-SEM analysis shown in Fig. 5.

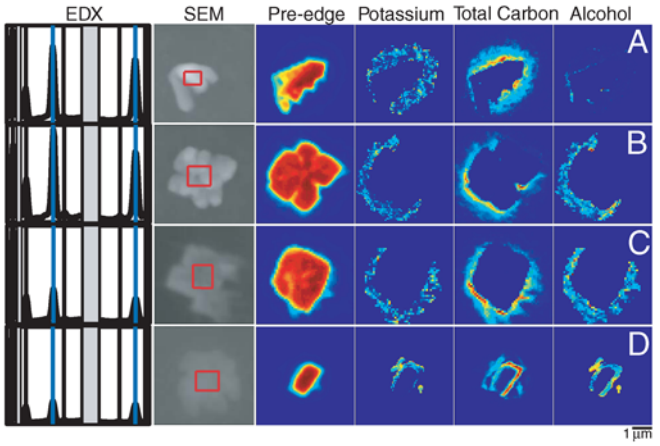

Fig. 5. SEM-EDX spectra and images and STXM-NEXAFS C and K images of individual particles from ICEALOT and VOCALS-REx, illustrating organic coatings on crystallized NaCl. From left to right, each row shows "EDX" spectra, with absorption lines for C, O, N, Na (*blue*), Mg, Si (not shown because of substrate interference), S, primary Cl (*blue*), and secondary Cl; "SEM" image, with red box showing the region over which the EDX spectrum was averaged; "Pre-edge" of C by STXM-NEXAFS showing the particle regions that absorb before the C edge, which includes most atoms other than C; "Potassium" of STXM-NEXAFS showing the K containing particle regions; "Total Carbon" of STXM-NEXAFS showing the C-containing regions; "Alcohol" of STXM-NEXAFS (integrated from 289.3–289.5 eV) showing the organic hydroxyl containing regions. The particles shown in (*A*) and (*B*) are sampled during an unassigned time at the south end of the Arctic samples while the ship was north of Iceland, indicated by the marker in Fig. 4 at 71.5 N, 7.6 W on April 20, 2008 from 11:13 to 11:46; the particle in (*C*) was collected in Arctic air masses during ICEALOT indicated by the marker in Fig. 4 at 79.3 N, 9.2 E on April 15, 2008 from 13:26 to 13:36; the particle in (*D*) is collected during VOCALS-REx at 21.0 S, 82.9 W in a clean marine air mass on November 28, 2008 from 16:00 to 16:50.

inclusions with high noncarbonaceous optical depth. Analysis by SEM revealed similar types of cuboidal structures (including aggregates of smaller cuboids), illustrated in Fig. 5, identified as primarily C, Na, and Cl with trace amounts of other sea salt elements (S, Mg). The cuboidal shapes are consistent with the crystallization of NaCl from an organic sea salt solution (28). It is not surprising that NaCl would crystallize at both the dry, cold conditions of the ICEALOT campaign (typically $<10\%$ relative humidity and $<0\,^{\circ}\mathrm{C}$) and during cold storage or SEM analysis in vacuum. STXM-NEXAFS analysis of the same particles shown in Fig. 5 also revealed cuboidal inclusions, within which the non-carbon (pre-edge) components saturated the signal and could not be quantified (consistent with crystalline NaCl). All of these particles contained detectable organic hydroxyl peaks at 289.4 eV in the regions surrounding the NaCl cuboids. Many of the particles also included small amounts of K, a sea salt component that is easily measured as part of NEXAFS C analysis; the distribution of C and K typically coincided and appeared to be homogeneously mixed in the edge regions surrounding the cuboidal structures, suggesting that the K and C components remained in an aqueous phase after NaCl crystallized. The thin homogeneous layers and aqueous phase of these organic compounds indicates properties similar to carbohydrates and other DOC rather than POC.

Discussion

The ICEALOT results identify marine organic contributions of $0.1-0.4\ \mu g\,m^{-3}$ that typically include 88% of the organic mass as organic hydroxyl groups. This percentage is consistent with the 80% carbohydrates in oceanic DOC (20). Similar marine organic signatures were identified in springtime measurements in the Southeastern (SE) Pacific Ocean near Chile during VOCALS-REx and wintertime measurements on the northern coast of Alaska at Barrow in air masses from clean marine regions, as summarized in Fig. 1. In addition to these two projects, two coastal [International Consortium for Atmospheric Research on Transport and Transformation (ICARTT)-Chebogue, ICARTT-Appledore] and two shipboard campaigns (ICARTT-R/V *Ronald Brown*, Texas Air Quality Study-R/V *Ronald Brown*) had sufficient marine emissions for similar factors to be resolved by PMF. Fig. 3 shows that the marine factors identified in these projects had similar calculated FTIR spectra as well as similar organic functional group compositions (illustrated by the pie charts) that provide a distinct contrast to the typical average compositions for other projects, shown in the pie charts of Fig. 1. The comparison illustrates important similarities in the FTIR spectral features in the organic hydroxyl absorption between 3,300 and 3,500 cm^{-1}, consistent with a large fraction of organic hydroxyl groups from marine saccharides emitted on sea salt particles. The minor differences among the FTIR spectra of the $OM1_{sea}$ derived in each project may indicate regional differences in the chemical composition of sea surface components (12, 29) or contamination from continental sources in the marine factors for projects where marine and continental sources were too comingled to be resolved during the project (27). Because ICEALOT has some of the largest fractions of OM1 and PM1 from marine sources, we use the correlations of $OM1_{sea}$ with Na1, wind speed, and number mean diameter to evaluate the two factors that clearly influence the production of marine particles: Wind speed and surface seawater composition. Given the similarities of marine particle organic compositions in other regions, we expect that the same mechanisms we identify for ICEALOT may apply in other regions.

Marine Particle Production. The correlations of organic hydroxyl groups with Na1 and wind speed at 18 m above sea level (u_{18}) as well as the SEM and STXM results showing organic layers on salt particles provide substantial evidence for the incorporation of DOC into homogenous bubble films at the ocean surface and subsequent emission into the atmosphere. The correlations between the $OM1_{sea}$ and wind speed (in Fig. 2*D*) when the North Atlantic and Arctic regions are combined yields the relationship

$$\mathbf{OM1_{sea} = 0.027\,u_{18} - 0.058} \qquad \mathbf{[1]}$$

($r = 0.90$ for North Atlantic and Arctic) for $OM1_{sea}$ in $\mu g\,m^{-3}$ and u_{18} in $m\,s^{-1}$. Whereas the concentration of NaCl in seawater is relatively invariant, DOC, POC, and TOC concentrations in the sea surface microlayer (SML) and subsurface water (SSW) vary regionally (as summarized in Fig. 6). If DOC affects the film concentration at rupture, then regional differences in surface seawater composition may contribute to creating particles of different diameters. To generalize, SSW ratios of TOC to Na are typically 10^{-4} to 10^{-3}, whereas aerosol-phase ratios of $OC1_{sea}$ to Na1 are 10^{-1} to 1. If the SML is enriched by up to a factor of 10 relative to the SSW (29), then aerosol enrichment factors of 10^2 to over 10^3 of marine organic compounds relative to NaCl in sea salt particles suggests that during drainage of the film, DOC is preferentially found in the topmost film-forming layer and NaCl is preferentially drained back to the seawater. The factor-of-two difference in $OM1_{sea}$/Na1 between the Arctic and North Atlantic regions could result from local differences in SML enrichment caused by sea state, frost flower particles, or biological gradients.

Marine Particle Diameter. As predicted and observed, the fraction of condensation nuclei that can serve as CCN increases with the number mean diameter of the particle distribution for constant chemical composition. These particles are mostly in the accumulation mode, and in ICEALOT the peak in number occurs

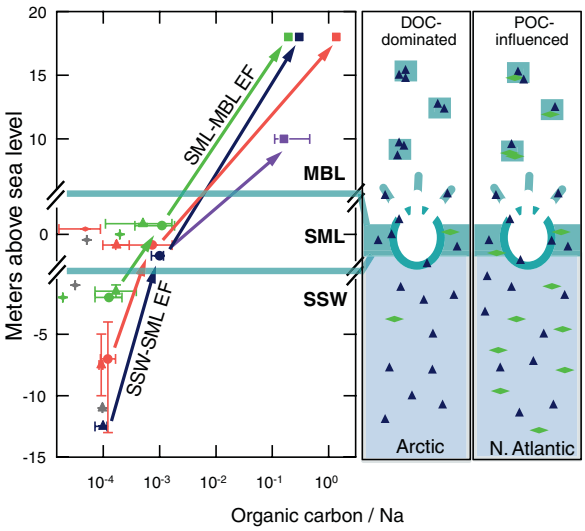

Fig. 6. Comparison of atmospheric and seawater ratios of organic carbon for the surface microlayer (SML) and $OC1_{sea}$ concentration in the marine boundary layer to Na1 concentration for Barrow Winter (*purple*), VOCALS-REx Southeast Pacific (*salmon*), ICEALOT North Atlantic (*chartreuse*), and ICEALOT Arctic (*dark blue*). SSW indicates subsurface water and MBL indicates marine boundary layer aerosol. The arrows show estimated MBL-SSW enrichment factors (EF) for each regional average aerosol $OC1_{sea}$/Na1 based on measurements made previously in the same region for TOC/Na as listed in Table S4 [except for the Arctic where TOC is estimated based on Thurman et al. (29)], in which we note that seasonal differences are neglected: MBL-SSW EF are 174 (ICEALOT North Atlantic), 304 (ICEALOT Arctic), 160 (2008 Barrow summer), and 1843 (VOCALS SE Pacific). The cartoons on the right illustrate the differing amounts of POC and DOC that contribute to particle formation from bubble bursting in the Arctic and North Atlantic regions.

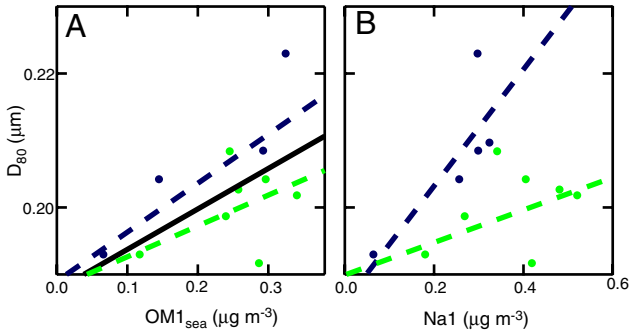

Fig. 7. Dependence of D_{80} on (*A*) $OM1_{sea}$ and (*B*) Na1 for the Arctic (*dark blue*) and North Atlantic (*chartreuse*) air masses. Correlation coefficients for the linear fits (colored dashed lines) of D_{80} are 0.59 and 0.49 for $OM1_{sea}$ and 0.86 and 0.48 for Na1, both for the Arctic and North Atlantic, respectively. The solid black line in (*A*) shows the fit for both sectors, given in Eq. [2].

between 100 and 300 nm. The number mean diameter of this mode is often defined for particles <80 nm, D_{80}, as this lower bound typically tracks the Hoppel minimum and has been used as a proxy for CCN in marine conditions (2). The production of particles from bubbling as part of a sea spray mode at this size is supported by laboratory bubbling experiments (30–32). During ICEALOT D_{80} varied from 140–240 nm, with an intermodal minimum usually occurring near 80 nm. The D_{80} range in the North Atlantic and Arctic regions was more limited, from 180–220 nm. There was no evidence for the third "forced bursting" mode or shoulder near 300 nm observed in laboratory experiments by Sellegri et al. (32). In the North Atlantic, D_{80} was mildly correlated ($r = 0.61$) to $OM1_{sea}$ and weakly correlated ($0.40 < r < 0.50$) to Na1 as shown in Fig. 7, with correlations to wind speed and marine particle mass given in Table S3. In the Arctic, D_{80} was strongly correlated ($r > 0.75$) to $OM1_{sea}$, Na1, wind speed, and marine particle mass. The correlation to wind speed is expected to result from the increased number and volume of trapped bubbles, resulting in additional bursting which lofts more particle mass. Whereas there are slight differences in slope (see Fig. 7 caption), both regions are reasonably fit by the same line

$$\mathbf{D_{80} = 0.060[OM1_{sea}] + 0.19} \qquad \mathbf{[2]}$$

($r = 0.70$ for North Atlantic and Arctic) although regional differences merit further consideration (*SI Text*).

The stronger correlations of D_{80} with $OM1_{sea}$ than with wind speed and the increase of D_{80} with $OM1_{sea}$/Na1 ($r = 0.46$ for the North Atlantic) corroborates the observed increase of number mean diameter with ion solution concentration observed in laboratory experiments for three values of salinity by Martensson et al. (30), which was later generalized for three types of salt solutions by Russell and Singh (31), and could be extended to allow for dissolved organic compounds as additional solutes. The physical mechanism controlling particle size is that the more concentrated solutions form film drops of similar size to the less concentrated solutions (because the latter is controlled by the thickness at which the film ruptures)—but containing a larger mass of ionic and organic solutes—which upon drying to equilibrium in the atmosphere result in larger particles. The second order effects of surface tension and density changes to the solution properties will also contribute to the particle diameter, after the threshold concentration has been exceeded (31).

Concluding Remarks. We have presented results that show the majority of organic mass in clean regions of the North Atlantic and Arctic was composed of carbohydrate-like compounds containing organic hydroxyl groups from primary emissions of the ocean. For the ICEALOT campaign, this conclusion is based on (*i*) the preponderance of organic hydroxyl group mass concentrations in the cleaner conditions measured in the North Atlantic and Arctic air masses, (*ii*) their correlation with Na concentrations, (*iii*) their correlation with wind speed, (*iv*) the large organic hydroxyl group composition of a PMF-based marine factor, which correlates with Na concentrations and wind speed, (*v*) spatial correlations of potential source locations with ocean regions, and (*vi*) single particle evidence of organic components surrounding NaCl. We have also shown a correspondence of the marine factor with FTIR spectra for a set of saccharide standards as reference compounds for marine carbohydrates. These spectral similarities extend to marine factors derived from observations in additional marine-influenced campaigns, including VOCALS-REx and Barrow. The consistency of these trends in diverse regions and the significant fraction of organic and particle mass for which the marine organic hydroxyl groups account demonstrate broad evidence for a causal connection between seawater organic components and marine particle components. Both the magnitude of the organic mass contribution of $0.1 - 0.4$ μg m^{-3} and its association with the carbohydrate signature of organic hydroxyl functional groups provide strong evidence for primary marine organic contributions to submicron atmospheric particles.

To quantify the contribution of the observed primary marine organic mass for atmospheric aerosol models, we have shown that during ICEALOT wind speed is a good predictor of $OM1_{sea}$, despite regional variability in seawater organic concentrations. The <500 nm diameter of the marine particles and the apparent solubility of the carbohydrate-like components in an aqueous phase suggests that DOC provides the source of most $OM1_{sea}$, although in bloom conditions in productive waters POC could also contribute (11). DOC in the sea surface microlayer may also increase the mean diameter of marine particles by incorporating

more soluble nonaqueous components in bubble film at the critical thickness (31). Given the sensitivity of aerosol–cloud interactions to the size of accumulation mode marine particles, seawater organic compounds may play an important role in climate by affecting cloud drop formation and albedo. Whereas the multivariate nature and regional variability of the bubble-bursting particle production mechanism cannot be addressed comprehensively in one study, the proposed role of marine organic components discussed here may provide a starting point for improving aerosol representation in global climate models until more comprehensive studies can be undertaken.

Materials and Methods

Organic particles were measured by the three complementary techniques of FTIR, Quadropole Aerosol Mass Spectrometry (Aerodyne Inc.), and STXM-NEXAFS, all of which are described in detail for prior studies (33, 34) and for ICEALOT specifically in *Supporting Information*. CCN (Droplet Measurement Technologies) and submicron number size distributions by mobility (TSI) were also collected. To identify the types of components present in particles, we have employed standard techniques for PMF and PSCF, as described in *Supporting Information*.

ACKNOWLEDGMENTS. We thank Satoshi Takahama and Shang Liu for carrying out the analysis of ICEALOT particles by STXM-NEXAFS with the advice of David Kilcoyne at Beamline 5.3.2 of the Advanced Light Source of the Lawrence Berkelye National Laboratory. Doug Day, Patrick Shaw, and Ashley Corrigan assisted in the measurements of standards and comparisons to literature and satellites. Collection of FTIR and STXM-NEXAFS samples was partially supported by a gift from the Clean Air Task Force. The analyses reported here were supported by National Science Foundation Grant ATM-0744636.

1. Haywood JM, Roberts DL, Slingo A, Edwards JM, Shine KP (1997) General circulation model calculations of the direct radiative forcing by anthropogenic sulfate and fossil-fuel soot aerosol. *J Climate*, 10(7):1562–1577.
2. Clarke AD, Owens SR, Zhou JC (2006) An ultrafine sea-salt flux from breaking waves: Implications for cloud condensation nuclei in the remote marine atmosphere. *J Geophys Res*, 111(D6):10.1029/2005JD006565.
3. Spracklen DV, Arnold SR, Sciare J, Carslaw KS, Pio C (2008) Globally significant oceanic source of organic carbon aerosol. *Geophys Res Lett*, 35(L12811):10.1029/2008GL033359.
4. Randles CA, Russell LM, Ramaswamy V (2004) Hygroscopic and optical properties of organic sea salt aerosol and consequences for climate forcing. *Geophys Res Lett*, 31(L16108):10.1029/2004GL020628.
5. Ming Y, Russell LM (2001) Predicted hygroscopic growth of sea salt aerosol. *J Geophys Res*, 106(D22):28259–28274.
6. Ming Y, Russell LM (2004) Organic aerosol effects on fog droplet spectra. *J Geophys Res*, 109(D10206):10.1029/2003JD004427.
7. Gagosian RB, Zafiriou OC, Peltzer ET, Alford JB (1982) Lipids in Aerosols from the Tropical North Pacific—Temporal Variability. *J Geophys Res*, 87(NC13):11 133–111 144.
8. Aller JY, Kuznetsova MR, Jahns CJ, Kemp PF (2005) The sea surface microlayer as a source of viral and bacterial enrichment in marine aerosols. *J Aerosol Sci*, 36(5-6):801–812.
9. Cavalli F, et al. (2004) Advances in characterization of size-resolved organic matter in marine aerosol over the North Atlantic. *J Geophys Res*, 109(D24215):10.1029/2004JD005137.
10. Crahan KK, et al. (2004) Speciation of organic aerosols in the tropical mid-pacific and their relationship to light scattering. *J Atmos Sc*, 61(21):2544–2558.
11. Facchini MC, et al. (2008) Primary submicron marine aerosol dominated by insoluble organic colloids and aggregates. *Geophys Res Lett*, 35(L17814):10.1029/2008GL034210.
12. Gogou AI, Apostolaki M, Stephanou EG (1998) Determination of organic molecular markers in marine aerosols and sediments: One-step flash chromatography compound class fractionation and capillary gas chromatographic analysis. *J Chromatogr A*, 799(1-2):215–231.
13. Kuznetsova M, Lee C, Aller J (2005) Characterization of the proteinaceous matter in marine aerosols. *Mar Chem*, 96(3-4):359–377.
14. Leck C, Bigg EK (2005) Source and evolution of the marine aerosol—A new perspective. *Geophy Res Lett*, 32(19):10.1029/2005GL023651.
15. Mochida M, Kitamori Y, Kawamura K, Nojiri Y, Suzuki K (2002) Fatty acids in the marine atmosphere: Factors governing their concentrations and evaluation of organic films on sea-salt particles. *J Geophys Res*, 107(D17):10.1029/2001JD0.
16. O'Dowd CD, et al. (2004) Biogenically driven organic contribution to marine aerosol. *Nature*, 431(7009):676–680 10.1038/nature02959.
17. Sicre MA, Peltzer ET (2004) Lipid geochemistry of remote aerosols from the southwestern Pacific Ocean sector. *Atmos Environ*, 38(11):1615–1624 10.1016/j.atmosenv.2003.12.012.
18. Langmann B, Scannell C, O'Dowd C (2008) New directions: Organic matter contribution to marine aerosols and cloud condensation nucleistar. *Atmos Env*, 42(33):7821–7822.
19. Facchini MC, et al. (2008) Important Source of Marine Secondary Organic Aerosol from Biogenic Amines. *Environ Sci Technol*, 42(24):9116–9121 10.1021/es8018385.
20. Aluwihare LI, Repeta DJ, Chen RF (1997) A major biopolymeric component to dissolved organic carbon in surface sea water. *Nature*, 387(6629):166–169.
21. Aluwihare LI, Repeta DJ (1999) A comparison of the chemical characteristics of oceanic DOM and extracellular DOM produced by marine algae. *Mar Ecol Prog Ser*, 186:105–117.
22. Gilardoni S, et al. (2007) Regional variation of organic functional groups in aerosol particles on four US east coast platforms during the International Consortium for Atmospheric Research on Transport and Transformation 2004 campaign. *J Geophys Res*, 112(D10):10.1029/2006JD007737.
23. Maria SF, et al. (2003) Source signatures of carbon monoxide and organic functional groups in Asian Pacific Regional Aerosol Characterization Experiment (ACE-Asia) submicron aerosol types. *J Geophys Res*, 108(D23):10.1029/2003JD003703.
24. Pelzer ET, Alford JB, Gagosian RB (1984) *Methodology for sampling and analysis of lipids in aerosols from the remote marine atmosphere* (Woods Hole Oceanographic Inst, Woods Hole), in Technical Report 84-9.
25. O'Dowd CD, Smith MH (1993) Physico-chemical properties of aerosol over the North East Atlantic: Evidence for wind speed related sub-micron sea-salt aerosol production. *J Geophys Res*, 98:1137–1149.
26. Monahan EC, Omuircheartaigh IG (1986) Whitecaps and the Passive Remote-Sensing of the Ocean Surface. *Int J Rem Sens*, 7(5):627–642.
27. Russell LM, et al. (2009) Oxygenated fraction and mass of organic aerosol from direct emission and atmospheric processing measured on the R/V Ronald Brown during TEXAQS/GoMACCS 2006. *J Geophys Res*, 114 10.1029/2008JD011275.
28. Laskin A, Cowin JP, Iedema MJ (2006) Analysis of individual environmental particles using modern methods of electron microscopy and X-ray microanalysis. *J Electron Spectrosc Relat Phenom*, 150(2-3):260–274 10.1016/j.elspec.2005.06.008.
29. Thurman EM (1985) *Organic geochemistry of natural waters (Developments in biogeochemistry)* (Springer, New York), 1st Ed (April 30, 1985) p 516.
30. Martensson EM, Nilsson ED, de Leeuw G, Cohen LH, Hansson HC (2003) Laboratory simulations and parameterization of the primary marine aerosol production. *J Geophys Res*, 108(D9):10.1029/2002JD002263.
31. Russell LM, Singh EG (2006) Submicron salt particle production in bubble bursting. *Aerosol Sci Tech*, 40(9):664–671 10.1080/02786820600793951.
32. Sellegri K, O'Dowd CD, Yoon YJ, Jennings SG, de Leeuw G (2006) Surfactants and submicron sea spray generation. *J Geophys Res*, 111(D22):10.1029/2005JD006658.
33. Russell LM, Maria SF, Myneni SCB (2002) Mapping organic coatings on atmospheric particles. *Geophys Res Lett*, 29(16):10.1029/2002GL014874.
34. Takahama S, Gilardoni S, Russell LM, Kilcoyne ALD (2007) Classification of multiple types of organic carbon composition in atmospheric particles by scanning transmission X-ray microscopy analysis. *Atmos Environ*, 41(40):9435–9451 10.1016/j.atmosenv.2007.08.051.